

2002

# Recent results from the in situ study of hydrothermal crystallizations using time-resolved X-ray and neutron diffraction methods

Richard I. Walton

Alexander J. Norquist

*Haverford College*, [anorquis@haverford.edu](mailto:anorquis@haverford.edu)

Ronald I. Smith

Dermot O'Hare

Follow this and additional works at: [http://scholarship.haverford.edu/chemistry\\_facpubs](http://scholarship.haverford.edu/chemistry_facpubs)

---

## Repository Citation

Walton, Richard I., et al. "Recent results from the in situ study of hydrothermal crystallisations using time-resolved X-ray and neutron diffraction methods." *Faraday Discussions* 122 (2003): 331-341.

This Journal Article is brought to you for free and open access by the Chemistry at Haverford Scholarship. It has been accepted for inclusion in Faculty Publications by an authorized administrator of Haverford Scholarship. For more information, please contact [nmedeiro@haverford.edu](mailto:nmedeiro@haverford.edu).

---

# Recent results from the *in situ* study of hydrothermal crystallisations using time-resolved X-ray and neutron diffraction methods

---

Richard I. Walton,<sup>a</sup> Alexander Norquist,<sup>b</sup> Ronald I. Smith<sup>c</sup> and Dermot O'Hare<sup>\*b</sup>

<sup>a</sup> School of Chemistry, University of Exeter, Stocker Road, Exeter, UK EX4 4QD

<sup>b</sup> Inorganic Chemistry Laboratory, South Parks Road, Oxford, UK OX1 3QR.

E-mail: [dermot.ohare@chem.ox.ac.uk](mailto:dermot.ohare@chem.ox.ac.uk)

<sup>c</sup> ISIS Facility, Rutherford Appleton Laboratory, Chilton, Didcot, Oxon, UK OX11 0QX

Received 25th January 2002, Accepted 29th April 2002

First published as an Advance Article on the web 30th July 2002

We present new time-resolved powder diffraction data measured *in situ* during the hydrothermal crystallisation of two families of crystalline inorganic materials. In the first study, we have used time-resolved energy-dispersive X-ray diffraction (EDXRD) to follow the formation of zeolitic zinc phosphates from amine phosphates and zinc oxide in acidic solutions at 60–150 °C. The advantage of this method is the ability to penetrate a laboratory-sized reaction vessel and to measure data in short (< 1 min) time intervals. Integration of the Bragg peak intensities during the crystallisation of the product allows accurate crystallisation curves to be produced. In addition, in a number of cases, we observe the formation of transient crystalline intermediate phases which can be identified by use of a new three-element detector that allows a large amount of diffraction data to be measured during the experiment. We are thus able to show that three-dimensional zinc phosphate architectures often form *via* low-dimensional chain and layered phases, which is consistent with a recent *aufbau* model proposed for their formation. In the second study, we focus on the hydrothermal formation of ferroelectric barium titanate from TiO<sub>2</sub> and barium salts in alkaline solution using time-resolved neutron diffraction. Although the time resolution of the neutron diffraction experiment is lower than the EDXRD experiment (data are measured in intervals of 5 min), we are able to penetrate reaction mixtures that are highly absorbing towards X-rays, and thus can measure data in a large volume reaction cell. Neutron diffraction data were collected on one of the highest-flux/highest detector-coverage diffractometers currently available; the GEM diffractometer at ISIS, UK. These experiments reveal that BaTiO<sub>3</sub> crystallises after a large amount of TiO<sub>2</sub> has been consumed; this implies that a dissolution–crystallisation mechanism predominates. Additional mechanistic information is inferred by the observation of transient crystalline phases under certain reaction conditions.

---

## 1. Introduction: *in situ* diffraction studies of the hydrothermal formation of inorganic solids

The hydrothermal preparation of inorganic solids has become of increasing importance in the past few years. The term *hydrothermal* simply refers to the use of water heated above 100 °C in a sealed container as a reaction medium. Under these conditions a mild pressure is developed (typically up to 20 atm when temperatures of less than 250 °C and subcritical conditions are employed) and the solvent properties are rather different from those at ambient conditions.<sup>1</sup> The method has uniquely allowed the synthesis of a diversity of microporous, zeolitic solids, now containing elements from almost all groups of the Periodic Table, and offering a wide range of pore dimensions, with the added attraction of specific chemical activity brought about by the constituent elements.<sup>2</sup> The hydrothermal method has also been used, to a lesser extent, in the preparation of condensed inorganic phases, which are usually synthesised using high temperature ceramic routes.<sup>3</sup> In this case, the advantage of the hydrothermal route lies in the rapid mixing of reagents to form homogeneous products and in the control of particle size and morphology of the material produced.

The use of hydrothermal synthesis as a preparative method in solid-state inorganic chemistry is directed towards materials with practical application: microporous materials already find widespread use in shape-selective catalysis, ion-exchange and gas separation, and condensed inorganic solids have a diversity of important properties from negative thermal expansion and unusual elastic properties, to magnetic properties and superconductivity. One drawback of the use of hydrothermal synthesis at present is that the method is unable to allow a rational preparation of desired solid materials: the synthesis of new materials is somewhat of a black art with many experimental parameters to vary (such as temperature, time, fill of reaction vessel, choice of reagents *etc.*) by a trial and error approach until a new crystalline material is synthesised in a pure form.

It would be highly advantageous to have knowledge of the reaction mechanisms leading to the formation of crystalline solids under hydrothermal conditions: this would allow the outcome of new reactions to be predicted and control of particle size of the product could be achieved, vital for the optimisation of the properties of a material for commercial application. The complexity of these crystallisations, involving heterogeneous mixtures under elevated temperature and pressure, suggests that, to begin with, the mechanisms will be multi-step reactions, involving equilibria between many competing processes. Thus a large amount of kinetic and mechanistic data will be required to understand the reaction mechanisms. The major limitation on obtaining the required mechanistic data for hydrothermal reactions is that sealed, thick-walled reaction containers are employed, from which it is very difficult to make measurements of even extent of reaction in real time and thus to obtain the kinetic data. Several time-resolved powder diffraction experiments have in the past 7 years or so been developed to allow direct observation of the formation of crystalline solids under hydrothermal conditions.<sup>4</sup> These use either high-intensity synchrotron-generated X-ray beams that can penetrate steel cells, or neutron beams that are little scattered and absorbed by the cell material. Such experiments have become invaluable in developing our understanding of hydrothermal crystallisations, since it is possible to accurately measure crystallisation curves by determining the time dependence of the intensities of characteristic Bragg peaks of particular phases, and the observation of transient crystalline phases has also been possible. In this paper we illustrate the type of data that may currently be obtained using *in situ* powder diffraction by presenting some of our most recent results using state-of-the-art time-resolved X-ray and neutron diffraction methods for following hydrothermal reactions. Before describing the details of the time-resolved diffraction experiments, we will briefly introduce the two systems studied.

### The crystallisation of open-framework zinc phosphates

The zinc phosphates are part of a now large family of phosphate-based solids that have open-framework zeolitic structures. It was first shown for the aluminium phosphates in 1982 that zeolite analogue framework structures could be produced,<sup>5</sup> and since then metals from almost every group of the Periodic Table have been incorporated into the open-framework phosphates.<sup>2</sup> The importance of the phosphates is two-fold: (i) the ready inclusion of transition elements infers unusual catalytic properties, and (ii) novel framework architectures are possible based on polyhedral other

than the tetrahedral units found in zeolites (for example 5- and 6- coordinate gallium, and 3-coordinate trigonal Sn bipyramids). We have chosen to study the zinc phosphates since it has been postulated by Rao *et al.* that their formation takes place *via* the building up of three-dimensional structures from lower-dimensional structures (chain 1D phases and layered 2D phases).<sup>6</sup> This *aufbau* model for crystallisation requires experimental verification, and we have begun to investigate the syntheses of the zinc phosphates using *in situ* techniques to track changes in crystallinity in real time, with the aim of providing evidence for how crystallisation proceeds. The family of zinc phosphates is particularly attractive to study, because a large number of closely-related phases have been structurally characterised; we thus will be in a favourable position to identify any transient crystalline phases observed during an *in situ* study. In a preliminary *in situ* X-ray diffraction study of the formation of some of the zinc phosphates from amine phosphates, zinc oxide and dilute acid at 150 °C, we have already observed the formation of solids with low dimensional structures before the onset of crystallisation of three-dimensional, zeolitic frameworks.<sup>7</sup> In the current paper we present recent results from a further study of the zinc phosphate system to illustrate the use of time-resolved energy-dispersive X-ray diffraction.

### The hydrothermal crystallisation of barium titanate

Tetragonal barium titanate is the most widely used ferroelectric solid. Its high permittivity makes the material an excellent capacitor, and the solid is commonly used in electronic devices such as multilayer capacitors, thermistors, electro-optic devices and dynamic random access memories.<sup>8</sup> Although the synthesis of barium titanate using conventional solid state chemistry is straightforward, and simply involves the direct, stoichiometric solid-state reaction between titania and barium carbonate at ~900 °C, the method has two distinct disadvantages: (i) repeated cycles of sample regrinding and reheating are necessary to achieve sample homogeneity and (ii) control of particle size is extremely difficult to achieve, and often irregularly shaped particles of a wide particle-size distribution are formed. The hydrothermal preparation of barium titanate offers a very attractive alternative to the solid-state reaction, and has been proven to allow the rapid one-step route to homogeneous BaTiO<sub>3</sub> from distinct Ba and Ti precursors, and additionally allows the preparation of fine powders of the solid that consist of spherical particles ranging in size from nanometres to microns.<sup>9-11</sup> The control of particle size and morphology that the hydrothermal route offers is of great interest for two reasons: (i) for the preparation of ceramics with few grain boundaries by sintering the fine powders and (ii) in the chemical fabrication of miniaturised devices. For these reasons the hydrothermal crystallisation mechanism of barium titanate has been the focus of some attention in the past few years [see *e.g.* ref. 12 and 13]. All the previous kinetic studies, however, used data obtained by quenching hydrothermal reactions: material was removed from the reaction vessel after it had been cooled to room temperature when a prescribed period of heating time had elapsed. Such studies do provide useful information about the extent of reaction and changes in sample crystallinity with time, but rely on the assumption that the material recovered by quenching is the same as that present under reaction conditions, and has not undergone any irreversible change on cooling and isolation. In this paper we describe recent results from a time-resolved neutron diffraction study of hydrothermal barium titanate formation; this is part of a series of experiments we have performed on the system and is the first study to follow the reaction *in situ*.<sup>14,15</sup>

## 2. Time-resolved energy-dispersive X-ray diffraction studies of the formation of open-framework zinc phosphates

### 2.1. The energy-dispersive X-ray diffraction experiment

Station 16.4 of the Daresbury Synchrotron Radiation Source was used to perform time-resolved EDXRD measurements. Station 16.4 is a white-beam diffraction instrument that was constructed 7 years ago with the specific aim of providing an instrument for kinetic studies, and for measuring diffraction data from materials under extreme pressure, a situation that requires confined sample containers.<sup>16</sup> The most significant development in the past few years on Station 16.4 is the installation of a three-element, energy-discriminating, solid-state detector by Barnes *et al.*<sup>17</sup> This

device allows three (overlapping) regions of diffraction data to be measured simultaneously. In terms of following chemical reactions *in situ* the synchrotron EDXRD method offers three relevant experimental characteristics: (i) the incident X-ray flux is very high ( $\sim 10^{10}$  photons  $s^{-1}$ ), and this means firstly that data can be collected in extremely short periods of time (sub-second data collection is now possible), and secondly that penetration of thick-walled environmental sample containment is possible; (ii) all data are measured simultaneously by the energy-discriminating detector, which also minimises the data collection time; and (iii) the fixed-angle, energy-discriminating detector means that the path of X-rays through the sample container requires only narrow entrance and exit slits, which in turn allows real heating devices/pressure containers to be modified only slightly to allow the passage of the beam. The Oxford hydrothermal reaction cell has been described in some detail previously.<sup>18</sup> This apparatus is a large-volume hydrothermal reaction cell from which EDXRD data may be collected at up to 250 °C, typical of the temperatures used in hydrothermal synthesis. This reaction cell is virtually identical in design and construction to the 23 mL Parr hydrothermal autoclaves widely used in many research laboratories, but the steel walls of the cell are thinned to 0.3 mm to minimise absorption of X-rays.

In the current study, all chemicals were purchased from chemical companies and used as supplied: ZnO (Aldrich 99%), orthophosphoric acid,  $H_3PO_4$ , (BDH, 85% in water), 1,4-diazabicyclo[2.2.2]octane (DABCO),  $N_2C_6H_{12}$ , (Aldrich 98%), piperazine,  $N_2C_4H_{10}$ , (Aldrich 99%), *N,N,N',N'*-tetramethylethylenediamine,  $(CH_3)_2NCH_2CH_2N(CH_3)_2$ , (Aldrich 99.5%),  $ZnSO_4 \cdot 7H_2O$ , (Aldrich 99%), HCl (Fisher, 32% in water), methanol (Fisher).  $[C_6N_2H_{14}][HPO_4] \cdot H_2O$  (DABCO-P)<sup>19</sup> was synthesised by mixing 6.2 g (0.055 mol) of DABCO with 6.4 g  $H_3PO_4$ . 40 mL of methanol was added under stirring. A white precipitate was recovered by filtration.  $[C_4N_2H_{12}][HPO_4] \cdot H_2O$  (PIP-P)<sup>20</sup> was synthesised by dissolving 4 g (0.046 mol) piperazine in 40 mL of deionised water. A thick white precipitate formed immediately after the addition of 6.44 g  $H_3PO_4$ , and was recovered by filtration.  $[C_6N_2H_{18}][HPO_4] \cdot 2H_2O$  (TMED-P)<sup>21</sup> was synthesised by mixing 4.64 g (0.04 mol) of *N,N,N',N'*-tetramethylethylenediamine with 6.44 g  $H_3PO_4$ . The addition of 40 mL of methanol under stirring resulted in the immediate precipitation of a white powder.

## 2.2. Time-resolved EDXRD studies of the hydrothermal crystallisation of some zinc phosphates

This system was investigated using two synthetic approaches in an attempt to gain understanding of the crystallisation mechanisms and reaction kinetics. The first approach utilised the amine phosphate route,<sup>7,22</sup> while the second involved the transformation of a zinc phosphate monomer ( $[C_6N_2H_{18}][Zn(HPO_4)(H_2PO_4)_2]$ , ZPM-I)<sup>21</sup> to higher dimensionality structures. The first amine phosphate studied was piperazine phosphate (PIP-P).<sup>7</sup> It was observed that the one-dimensional ladder compound  $[C_4N_2H_{12}][Zn(HPO_4)_2(H_2O)]$ <sup>23</sup> is formed initially and then transforms to a series of three-dimensional phases;  $[C_4N_2H_{12}][Zn_{3.5}(PO_4)_3(H_2O)]$ ,  $[C_4N_2H_{12}][Zn_2(HPO_4)_2(H_2PO_4)_2]$  and  $[C_4N_2H_{12}][Zn(H_2O)Zn(HPO_4)(PO_4)]$ . In each reaction the PIP-P starting material is not observed owing to dissolution of this soluble species.<sup>7</sup>

Reactions involving another amine phosphate have also been conducted. Fig. 1 shows a stack plot of the time-resolved EDXRD data from the reaction of DABCO-P, zinc oxide, water and concentrated hydrochloric acid at 150 °C. No Bragg reflections were observed from the DABCO-P, suggesting that this starting material immediately dissolves under reaction conditions. After 12 min Bragg reflections from the three-dimensional open-framework material  $[C_6N_2H_{14}][Zn_2(HPO_4)_3]$  (ZnPO-DABCO-A)<sup>24</sup> are observed. These reflections increase in intensity for approximately an additional 55 min, at which point these peaks change in neither intensity nor position, Fig. 2. In this case we have not observed any low-dimensional precursor phases.

The second approach involves synthesising zinc phosphates from the zinc phosphate monomer, ZPM-I. The transformation of both ZPM-I and  $[C_6N_4H_{21}][Zn(HPO_4)_2(H_2PO_4)]$  (ZPM-II) to one, two and three-dimensional structures was recently reported by Rao *et al.* on the basis of *ex situ* studies whereby solid material was examined before and after reaction using laboratory powder diffraction.<sup>25</sup> Our initial *in situ* investigations have focussed on the formation of ZPM-I and its transformations in the presence of piperazine.

ZPM-I was synthesised by stirring a gel of composition  $ZnSO_4 \cdot 7H_2O$ :TMED-P:25  $H_2O$  at room temperature. Fig. 3 shows a stack plot of the time-resolved EDXRD data measured during

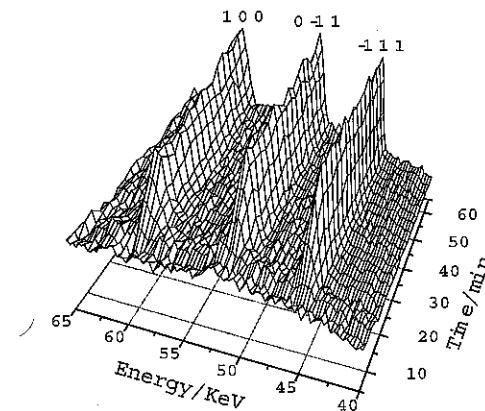


Fig. 1 A stack plot of EDXRD data measured during the crystallisation of ZnPO-DABCO-A from the reaction mixture ZnO:1.5 HCl:2 DABCO-P:50  $H_2O$ .

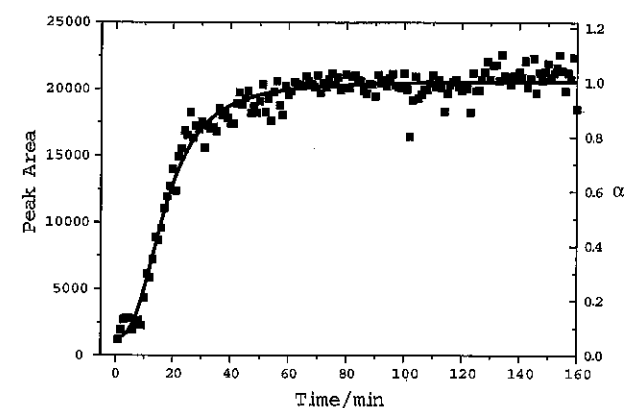


Fig. 2 Integrated peak areas of ZnPO-DABCO-A during crystallisation at 150 °C.

this process. No Bragg reflections were observed during the first 70 min at which point four characteristic reflections of ZPM-I increased in intensity during the next 30 min, until their intensity remained constant for the remainder of the experiment. The ZPM-I zinc phosphate monomer thus forms directly from solution with no transient crystalline phases detected.

The transformation of ZPM-I to higher dimensionality structures was investigated by reacting ZPM-I with piperazine in water at 60 °C. Fig. 4 shows a stack plot of the transformation of ZPM-I to ZnPO-PIP-I from a gel of composition ZPM-I:piperazine:275  $H_2O$ . ZPM-I is only observed during the first 5–6 min while ZnPO-PIP-I Bragg reflections are first detected in the seventh minute. After 20 min the reaction is complete and the ZnPO-PIP-I peak intensities remain constant. The precursor phase is almost completely consumed before the product is observed, which suggests that a solution mediated process is involved rather than a solid-state transformation. The decay of precursor phases and growth of products are expected to mirror one another if a solid-state mechanism is employed. These observations, only made possible by continual monitoring of the reaction under real conditions, provide the first pieces of information towards understanding the hydrothermal formation of these framework solids: we have observed in some cases the presence of a precursor low-dimensional phase prior to the crystallisation of 3D zeolitic phases, and have evidence that the transformation from 1D to 3D zinc phosphates is solution-mediated rather than a direct solid-state process.

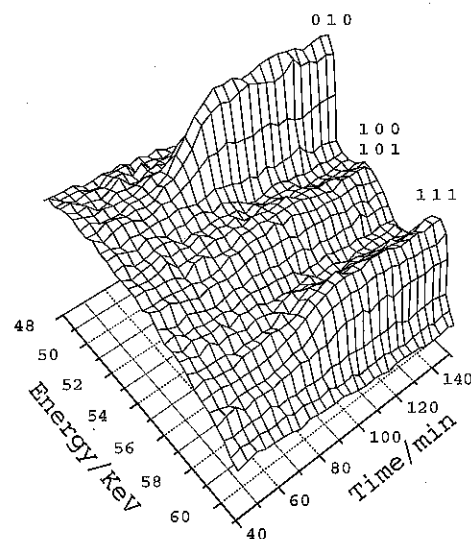


Fig. 3 A stack plot of EDXRD data measured during the crystallisation of ZPM-I.

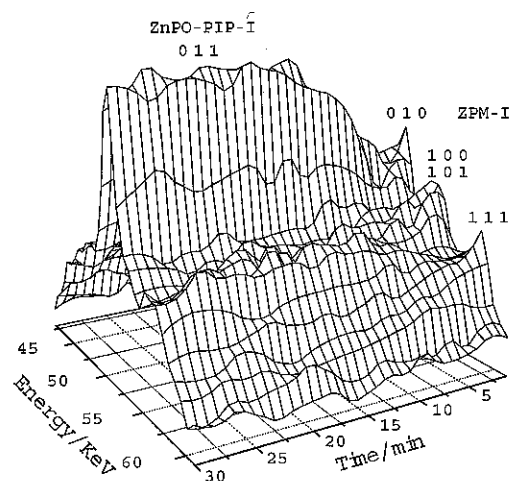


Fig. 4 A stack plot of EDXRD data measured during the transformation of ZPM-I to ZnPO-PIP-I at 60°C.

### 3. Time-resolved neutron diffraction studies of the hydrothermal formation of barium titanate

#### 3.1. A hydrothermal reaction cell for time-resolved neutron diffraction studies

We have described previously in some detail, the design, construction and use of a hydrothermal autoclave from which neutron diffraction data can be measured during the crystallisation of inorganic solids.<sup>26</sup> The apparatus was purposely designed to be of the same volume as the 23 mL Parr autoclaves widely used in many chemical laboratories; we are therefore simulating real reaction conditions in our *in situ* studies. Rather than being constructed from steel, as in the laboratory, the Oxford/ISIS reaction vessel is constructed from 0.3 mm thick “null scattering”

Ti–Zr alloy. This material contains Ti and Zr in such a proportion (67.7 atom% Ti and 32.3 atom% Zr) that the negative and positive neutron scattering lengths of Ti and Zr (–3.438 fm and 7.16 fm respectively) cancel completely, so that the average coherent scattering length is zero. The material is thus effectively invisible to neutrons. The alloy has similar mechanical properties to steel so is able to contain the pressure developed in a hydrothermal reaction. We experimented with different means of protecting the Ti–Zr alloy from the corrosive chemicals usually employed in a hydrothermal reaction, and found that Teflon<sup>®</sup>, usually used in the laboratory as an inert liner for hydrothermal autoclaves, gives rise to substantial scatter (both coherent and incoherent); instead the Oxford/ISIS cell is coated internally with a thin (~10 µm) layer of gold metal. The cell is heated top and bottom by cartridge heaters inserted into copper blocks, thus exposing a 4 cm high “window” to the neutron beam to which all sample in the reaction container is exposed. In essence our cell gives rise to minimal scattering in the neutron diffraction experiment, and so we are able to collect data from reacting mixtures of solids and liquids at elevated temperature and autogeneous without any contribution to the background from the cell.

Here we report recent data obtained using the Oxford/ISIS hydrothermal cell on one of the most recently constructed neutron diffractometers, the GEM (General Materials Diffractometer) at ISIS, the UK spallation neutron source.<sup>27</sup> GEM is a time-of-flight neutron diffractometer, with an extremely high detector coverage and count rate. Data are measured by a three-dimensional array of seven banks of high count-rate detectors. Combined with the relatively high neutron flux available on GEM, the high count rate means that GEM is ideally suited for time-resolved diffraction studies where data must be collected in short time intervals to maximise kinetic information.

#### 3.2. The hydrothermal crystallisation of barium titanate followed by neutron diffraction

We have previously presented some results on our study of hydrothermal barium titanate crystallisation.<sup>14,15</sup> Since our first studies, performed using the POLARIS diffractometer, the availability of new neutron diffractometers has greatly improved the quality of time-resolved data that we can obtain from the *in situ* experiment, and we have thus gained new insights into the steps involved in the hydrothermal formation of crystalline barium titanate. Using GEM we have now been able to reduce the time taken to record a useful diffraction pattern. With the POLARIS diffractometer we measured data in 15 min intervals; with GEM we can now acquire data in 5 min intervals. This has meant we can follow reactions that take place in shorter times than previously possible, and therefore we have been able to study the barium titanate crystallisation at higher temperatures. Fig. 5 shows a contour plot of data measured during the reaction between barium

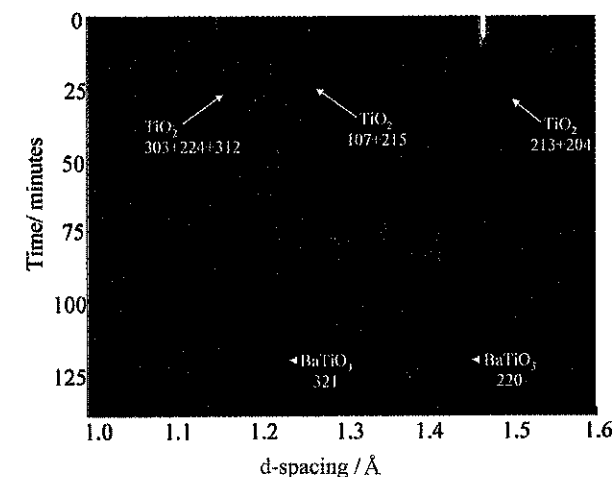


Fig. 5 A contour plot of neutron diffraction data measured during the crystallisation of BaTiO<sub>3</sub> from a mixture of composition 1.1BaCl<sub>2</sub>:TiO<sub>2</sub>:3.33 NaOD:16.7 D<sub>2</sub>O at 200°C. Pertinent Bragg peaks are marked.

chloride, BaCl<sub>2</sub> (10 g), titanium dioxide (anatase), TiO<sub>2</sub> (3.2 g), in a D<sub>2</sub>O solution of NaOD at 200 °C in the sealed hydrothermal cell. All chemicals were purchased from chemical companies and transferred to the hydrothermal cell under a flow of nitrogen to prevent aerial contamination and formation of BaCO<sub>3</sub>. Note that the use of deuterated reagents is required in the neutron diffraction experiment to minimise large backgrounds in the diffraction data due to incoherent scattering from protons. Even qualitative inspection of data such as these allows important observations to be made. For example, the time-scale of the reaction can be easily determined, something which would require probably several days worth of quenching and X-ray diffraction studies in order to estimate fractional crystallinity, and thus to obtain a crude crystallisation curve. In the case of this reaction, we can see that barium titanate begins to crystallise at ~20 min, and at ~40 min the crystallisation is complete, with no further increase in BaTiO<sub>3</sub> Bragg peak intensity apparent. A second important feature of these data is that they show that not only does the BaCl<sub>2</sub> starting material dissolve rapidly, but also that a significant amount of TiO<sub>2</sub> dissolves (or perhaps is transformed to an amorphous phase) before the onset of crystallisation of barium titanate.

Aside from qualitative observations, we can obtain quantitative information about the kinetics of crystallisation by determining the changing areas of Bragg reflections with time. Since the intensity of Bragg peaks is directly proportional to the amount of substance giving rise to the diffraction, their changing areas with time, allow a crystallisation curve to be calculated. Fig. 6 shows a crystallisation curve of BaTiO<sub>3</sub> produced by analysis of the 310 peak of BaTiO<sub>3</sub> and also shown are decay curves for both BaCl<sub>2</sub>, and TiO<sub>2</sub> similarly derived. The intensity data have been normalised to the maximum intensity of the Bragg peak in question. These data convincingly show how a TiO<sub>2</sub> Bragg peak intensity begins to decrease immediately on heating, and how a large amount of the crystalline TiO<sub>2</sub> is consumed before BaTiO<sub>3</sub> crystallises; a vital piece of information for establishing the crystallisation mechanism (see below). We also note that some of the TiO<sub>2</sub> does not either dissolve or react in the time the reaction was studied; this is consistent with previous observations that an excess of Ba is always required for the reaction to reach completion.<sup>12</sup>

Additional mechanistic information has been obtained by studying the barium titanate crystallisation at a variety of temperatures. For example, at 125 °C, transient Bragg peaks are observed at higher *d*-spacings. Fig. 7 shows data from detector bank 6 during this process and two distinct diffraction features can be observed to increase in intensity after the dissolution of BaCl<sub>2</sub> and then to decay more slowly as BaTiO<sub>3</sub> forms. Fig. 8 shows a narrower *d*-spacing range of three representative diffraction patterns measured during this time. The two transient diffraction peaks at ~2.53 Å and 2.71 Å, are, alone, extremely difficult to assign unambiguously. A likely candidate responsible for this phase is Ba<sub>2</sub>TiO<sub>4</sub>; this does exhibit strong Bragg peaks in the same region. Unfortunately, the expected most intense Bragg peak of Ba<sub>2</sub>TiO<sub>4</sub>, the 103 at 3.05 Å overlaps with strong diffraction features of both the BaCl<sub>2</sub> starting material and TiO<sub>2</sub>, ruling out confirmation of

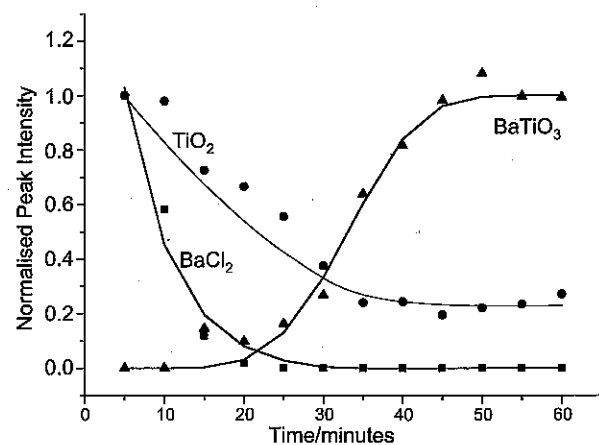


Fig. 6 Normalised integrated Bragg peak intensities obtained during the hydrothermal crystallisation of BaTiO<sub>3</sub> at 200 °C. Lines are guides to the eye and have no physical significance.

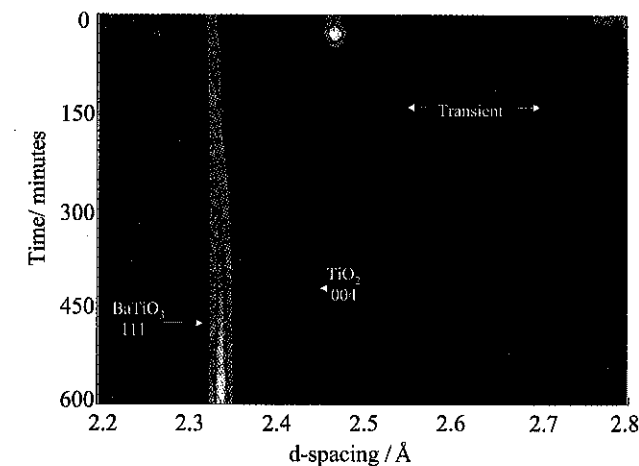


Fig. 7 A contour plot of neutron diffraction data measured during the crystallisation of BaTiO<sub>3</sub> from a mixture of composition 1.1 BaCl<sub>2</sub>:TiO<sub>2</sub>:3.33 NaOD:16.7 D<sub>2</sub>O at 125 °C.

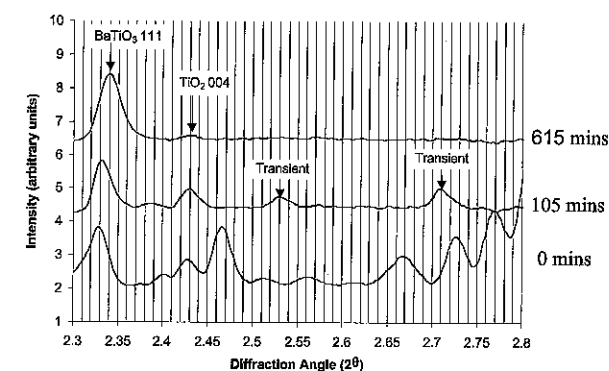


Fig. 8 Selected diffraction patterns recorded during the crystallisation of BaTiO<sub>3</sub> from a mixture of composition 1.1 BaCl<sub>2</sub>:TiO<sub>2</sub>:3.33 NaOD:16.7 D<sub>2</sub>O at 125 °C.

our phase assignment. Interestingly Bondioli *et al.* previously reported the presence of Ba<sub>2</sub>TiO<sub>4</sub> during the formation of BaTiO<sub>3</sub> in a conventional solid-state reaction.<sup>28</sup> Further experimental evidence is necessary to aid identification of the intermediate material we have observed, but at present we note that the kinetic crystallisation of a barium-rich barium titanate is consistent with a solution rich in Ba<sup>2+</sup> at the early stages of reaction.

We are able now to postulate that the hydrothermal formation of barium titanate occurs predominantly *via* a dissolution–crystallisation mechanism; the dissolution of both the barium-containing and titanium-containing reagents permits crystallisation directly from solution. This is consistent with our observation of the disappearance of a large amount of TiO<sub>2</sub> before the crystallisation of BaTiO<sub>3</sub>. The new results we have presented here, collected using the GEM diffractometer, compare very favourably with parallel studies we have performed using the constant wavelength diffraction D20 at the ILL.<sup>15</sup> In those studies we were also able to measure diffraction data in intervals of 5 min by virtue of a combination of high incident neutron flux and a 160° position-sensitive detector with rapid data acquisition. The quality of neutron diffraction data obtained using the two diffractometers is comparable, and we have already described the use of the D20 data to obtain rate constants for crystallisation at a number of temperatures, and thus an activation energy for what we believe to be nucleation-controlled crystal growth.<sup>15</sup> Our new corroborative results provide independent evidence for our earlier deductions. Our description of the

reaction mechanism as predominantly occurring *via* dissolution of all starting materials is important, since some authors have assumed an alternative heterogeneous-transformation mechanism in which solution Ba<sup>2+</sup> ions react with solid TiO<sub>2</sub> particles.<sup>12</sup>

#### 4. Conclusions

The two *in situ* studies that we have described in this paper demonstrate the quality of time-resolved diffraction data that currently may be obtained during the crystallisation of inorganic solids under hydrothermal conditions. There now exists a number of specially designed reaction cells for tracking hydrothermal crystallisations using time-resolved diffraction,<sup>4</sup> but our two methods are unique in that laboratory-sized reaction vessels are employed. We therefore study crystallisation under real conditions, and avoid the problems of accurately selecting the correct amounts of starting materials and of achieving reproducibility that might arise if reactions are scaled down to very small volumes. The time-resolved EDXRD method has the advantage of rapid data collection, but a disadvantage in the intrinsically low resolution of the diffraction data. In contrast, the time-resolved neutron diffraction technique offers high resolution diffraction data but lower time resolution (largely due to the fact that the incident neutron flux is considerably lower than that available from X-ray sources). The additional benefit of the time-resolved neutron method is the ability to study reacting mixtures that are highly absorbing towards X-rays (*i.e.* samples that contain high atomic number elements, such as barium).

The results of our time-resolved diffraction studies allow us, for the first time, to build up a picture of the events involved in the nucleation and crystallisation of inorganic materials under hydrothermal conditions. Before a complete reaction mechanism can be put forward, however, experimental results from other techniques need also to be considered. For example, because our time-resolved diffraction studies only detect changes in crystalline material in the hydrothermal reaction vessel and none of the amorphous phases present is probed, the data from spectroscopic methods, which do reveal changes on a local atomic scale, must also be considered. To this end, both NMR<sup>29</sup> and EXAFS<sup>30</sup> spectroscopies have been utilised by other workers to follow hydrothermal crystallisations. Such methods do allow the local atomic environment of specific atom types to be tracked selectively from starting material through any amorphous phases, and small particles of solid (that are too small to be detected by Bragg diffraction). It should be noted that time-resolved diffraction experiments of hydrothermal crystallisation will always be necessary to correlate changes in local atomic structure with the presence of crystalline materials, and thus, we believe, will be at the centre of the ongoing research into understanding how inorganic solids crystallise under hydrothermal conditions.

#### Acknowledgements

We thank the EPSRC for funding this work, Dr D. J. Taylor for his assistance with running the synchrotron experiments, and Dr P. Radaelli for help with configuring GEM for the neutron studies.

#### References

- 1 A. Rabeneau, *Angew. Chem. Int. Ed. Engl.*, 1985, **24**, 1026.
- 2 A. K. Cheetham, G. Férey and T. Loiseau, *Angew. Chem. Int. Ed. Engl.*, 1999, **38**, 3268.
- 3 G. Demazeau, *J. Mater. Chem.*, 1999, **9**, 15.
- 4 R. I. Walton and D. O'Hare, *Chem. Commun.*, 2000, 2283.
- 5 S. T. Wilson, B. M. Lok, C. A. Messina, T. R. Cannan and E. M. Flannigan, *J. Am. Chem. Soc.*, 1984, **106**, 6092.
- 6 C. N. R. Rao, S. Natarajan, A. Choudhury, S. Neeraj and A. A. Ayi, *Acc. Chem. Res.*, 2001, **34**, 80.
- 7 R. I. Walton, A. J. Norquist, S. Neeraj, S. Natarajan, D. O'Hare and C. N. R. Rao, *Chem. Commun.*, 2001, 1990.
- 8 G. H. Haertling, *J. Am. Ceram. Soc.*, 1999, **82**, 797.
- 9 P. K. Dutta and J. R. Gregg, *Chem. Mater.*, 1992, **4**, 843.
- 10 I. J. Clark, T. Takeuchi, N. Ohtori and D. C. Sinclair, *J. Mater. Chem.*, 1999, **8**, 83.
- 11 S. W. Lu, B. I. Lee, Z. L. Wang and W. D. Samuels, *J. Cryst. Growth*, 2000, **219**, 269.
- 12 J. O. Eckert, C. C. Hung-Houston, B. L. Gerstan, M. M. Lenka and R. E. Riman, *J. Am. Ceram. Soc.*, 1996, **79**, 2929.
- 13 I. MacLaren and C. B. Ponton, *J. Eur. Ceram. Soc.*, 2000, **20**, 1267.
- 14 R. I. Walton, R. I. Smith, F. Millange, I. J. Clark, D. C. Sinclair and D. O'Hare, *Chem. Commun.*, 2000, 1267.
- 15 R. I. Walton, F. Millange, R. I. Smith, T. C. Hansen and D. O'Hare, *J. Am. Chem. Soc.*, 2001, **123**, 12547.
- 16 R. L. Bilsborrow, N. Bliss, J. Bordas, R. J. Cernik, G. F. Clark, S. M. Clark, S. P. Collins, B. R. Dobson, B. D. Fell, A. F. Grant, N. W. Harris, W. Smith and E. Towns-Andrews, *Rev. Sci. Instrum.*, 1995, **66**, 1633.
- 17 P. Barnes, A. C. Jupe, S. L. Colston, S. D. Jacques, A. Grant, T. Rathbone, M. Miller, S. M. Clark and R. J. Cernik, *Nucl. Instrum. Methods Phys. Res. Sect. B*, 1998, **134**, 310.
- 18 J. S. O. Evans, R. J. Francis, D. O'Hare, S. J. Price, S. M. Clark, J. Flaherty, J. Gordon, A. Nield and C. C. Tang, *Rev. Sci. Instrum.*, 1995, **66**, 2442.
- 19 S. Neeraj, S. Natarajan and C. N. R. Rao, *Angew. Chem. Int. Ed. Engl.*, 1999, **38**, 3480.
- 20 D. Riou, T. Loiseau and G. Férey, *Acta Crystallogr., Sect. C*, 1993, **49**, 1237.
- 21 S. Neeraj, S. Natarajan and C. N. R. Rao, *J. Solid State Chem.*, 2000, **150**, 417.
- 22 S. Natarajan, S. Neeraj and C. N. R. Rao, *Solid State Sci.*, 2000, **2**, 87.
- 23 C. N. R. Rao, S. Natarajan and S. Neeraj, *J. Am. Chem. Soc.*, 2000, **122**, 2810.
- 24 W. T. A. Harrison, T. E. Martin, T. E. Gier and G. D. Stucky, *J. Mater. Chem.*, 1992, **2**, 75.
- 25 A. A. Ayi, A. Chourdury, S. Natarajan, S. Neeraj and C. N. R. Rao, *J. Mater. Chem.*, 2001, **11**, 1181.
- 26 R. I. Walton, R. J. Francis, P. S. Halasyamani, D. O'Hare, R. I. Smith, R. Done and R. Humphreys, *Rev. Sci. Instrum.*, 1999, **70**, 3391.
- 27 W. G. Williams, R. M. Ibberson, P. Day and J. E. Enderby, *Physica B*, 1998, **214-243**, 234.
- 28 K. Bondioli, A. Bonamartini-Corradi, A. M. Ferrari, T. Manfredini and G. C. Pellacani, *Mater. Sci. Forum*, 1998, **278-281**, 379.
- 29 F. Taulelle, M. Haouas, C. Gerardin, C. Estournes, T. Loiseau and G. Férey, *Colloids Surf. A*, 1999, **158**, 299.
- 30 G. Sankar, J. M. Thomas, F. Rey and G. N. Greaves, *J. Chem. Soc., Chem. Commun.*, 1995, 2549.